Cyanogen: structure, dynamics and inter-molecular potentials

1989 J. Phys.: Condens. Matter 1 5827

(http://iopscience.iop.org/0953-8984/1/34/001)

J. Phys.: Condens. Matter 1 (1989) 5827–5835. Printed in the UK

Cyanogen: structure, dynamics and inter-molecular potentials

B H Torrie† and B M Powell‡

† Guelph–Waterloo Program for Graduate Work in Physics, Waterloo Campus, University of Waterloo, Waterloo, Ontario, Canada N2L 3G1

‡ Atomic Energy of Canada Limited Research Company, Chalk River Nuclear Laboratories, Chalk River, Ontario, Canada K0J 1J0

Received 21 October 1988

Abstract. The crystal structure of cyanogen at 15 K has been determined using neutron powder profile measurements. This new structural information and the recently determined quadrupole moment have been included in revised calculations of the lattice dynamics. A satisfactory description of both the crystal structure and the dynamics cannot be obtained with any of the models used for the inter-molecular forces. The model giving the 'best' fit has potential parameters very different from those in the literature. The present results indicate that the concept of transferable potentials is not valid, at least in its simple form. Lattice frequencies, electrostatic interactions and low-temperature crystal structure data must all be included in the database if transferable, non-bonded, atom–atom potentials are to be a valid and useful concept.

1. Introduction

Cyanogen, N–C≡C–N, is a simple linear molecule which crystallises in the orthorhombic space group P*bca*, D_{2h}^{15} [1]. The structure is centrosymmetric and the relatively large unit cell contains four molecules. Since there are only two types of atom, there are only three inter-atomic potentials in cyanogen (C–C, N–N and C–N). Hence only a relatively small number of adjustable parameters are needed to describe the inter-atomic potentials—only nine in the model used here. Two additional parameters are needed to describe the electrostatic interactions. These parameters can be determined by fitting to six equilibrium conditions, the lattice energy, eight librational frequencies for modes that are Raman active and six translational frequencies for modes that are infrared active.

In earlier papers [2–4] the lattice dynamics of cyanogen was investigated but two vital pieces of information were lacking when these papers were written. The crystal structure at low temperatures, where a harmonic theory is applicable, and the value of the quadrupole moment were not known. We report here on the crystal structure at 15 K as determined by neutron powder profile measurements. The quadrupole moment of the gas phase has also recently been measured [5]. This new information has been included in revised calculations of the lattice dynamics. Particular attention has been paid to the importance of the electrostatic contribution to the lattice dynamics.

0953-8984/89/345827 + 09 $02.50

Table 1. The structural parameters of C_2N_2 at 15 K determined from the profile refinements. The bond lengths and bond angles were derived from the other fitted parameters. The R_i are defined as follows:

$$R_{\text{expected}} = \left(N \Big/ \sum_i \omega_i (y_i^{\text{obs}})^2\right)^{1/2} \qquad R_p = \sum_i |y_i^{\text{obs}} - y_i^{\text{calc}}| \Big/ \sum_i y_i^{\text{obs}}$$

$$R_{wp} = \left(\sum_i \omega_i (y_i^{\text{obs}} - y_i^{\text{calc}})^2 \sum_i \omega_i (y_i^{\text{obs}})^2\right)^{1/2}$$

$R_{\text{expected}}(\%)$			2.5
$R_p(\%)$			4.6
$R_{wp}(\%)$			6.0
Lattice parameters (Å)		a	6.2013(3)
		b	6.1509(3)
		c	7.0652(3)
Fractional coordinates and isotropic temperature factors (Å^2)	C	x	0.03081(3)
		y	−0.09199(4)
		z	0.04846(3)
		B	0.030(3)
	N	x	0.08345(3)
		y	−0.24507(3)
		z	0.12995(3)
		B	0.75(2)
Bond lengths (Å)	C–C		1.3768(3)
	C–N		1.1509(3)
Bond angle (deg)	C–C–N		179.6(2)

2. Experimental details

Cyanogen gas was supplied by Union Carbide, Canada, Ltd and a polycrystalline sample was prepared by cryogrinding the solid using the technique developed previously [6] for chlorine. The sample was contained in a thin-walled vanadium can in a Displex closed-cycle refrigerator at 15 K. It was rotated continuously throughout the measurements to minimise errors due to finite crystalline grain size. The diffraction measurements were made on the C5 triple-axis spectrometer, operating in the two-axis mode, at the NRU reactor, Chalk River. The monochromator was Si(115) and horizontal collimations of 0.44° and 0.20° were used before and after the sample respectively. A sapphire filter (5 cm long) was placed in the incident beam to reduce the flux of higher-order neutrons, and hence lower the background. The spectrometer was calibrated using Al powder as a standard and the neutron wavelength was determined to be 1.47977(2) Å. The experimental profiles were measured by stepping the detector in 0.1° steps from 20° to 119.6°. Typical counting times were ≃2 min per point.

3. Crystal structure analysis

The powder diffraction profiles were analysed by means of the program EDINP [7] which is a modification of the Rietveld analysis [8]. The observed peak shapes were well described by Gaussian profiles with full width at half height given by Γ where Γ^2 =

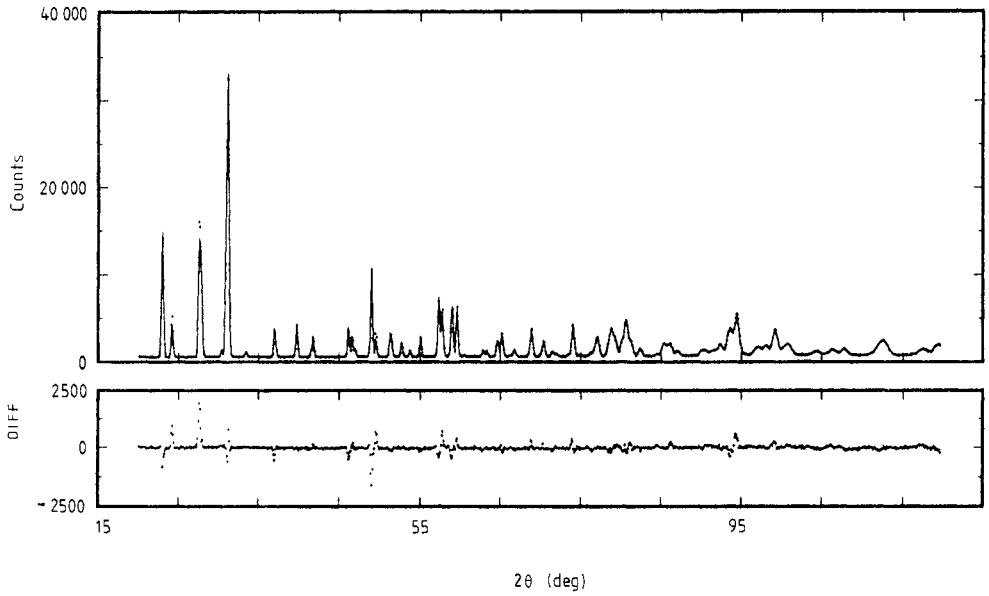

Figure 1. A comparison of the observed and calculated diffraction profiles of C_2N_2 at 15 K. The dots show the experimental intensities and the trace through them is the calculated intensity. The plot of DIFF against the scattering angle $2\theta_i$ is a quantitative measure of the discrepancies between the observed (y_i^{obs}) and calculated (y_i^{calc}) intensities at $2\theta_i$.

$U\tan^2\theta + V\tan\theta + W$ and 2θ is the scattering angle. Initial values of U, V and W were derived from the calibration procedure but the values were subsequently adjusted as part of the profile refinement. Since the structure was basically known from the x-ray structural determination [1], the analysis was reasonably straightforward. Initial values of the lattice parameters were calculated from the low-angle peak positions and positional parameters were taken from the earlier work [1]. Isotropic and anisotropic temperature factors were included in different refinements but the anisotropic temperature factors were found to be inconsistent with rigid-body motions. Furthermore, there were systematic differences between the observed and calculated peak intensities which indicated that there was preferred orientation in the sample. Therefore only isotropic temperature factors were included in the final refinements and a preferred orientation correction was applied based on the systematic discrepancies of the low-angle peaks. Finally, the value of the preferred orientation parameter was varied in steps until the best fit was obtained. The structural and thermal parameters determined from the final refinement are given in table 1. It should be noted that the isotropic thermal parameters have been corrected by $\Delta B = 0.22$ to allow for absorption in the sample [9]. Observed and calculated profiles are compared in figure 1, and the structure is shown in projection along the a axis in figure 2.

4. Discussion of the structure

The structure is similar to that found using x-rays [1] at a sample temperature of 178 K. Lowering the temperature to 15 K, as in the present experiment, reduced the unit-cell volume from 276.5 to 269.5 Å, a decrease of 2.5%. The a-axis length changed by −1.7%

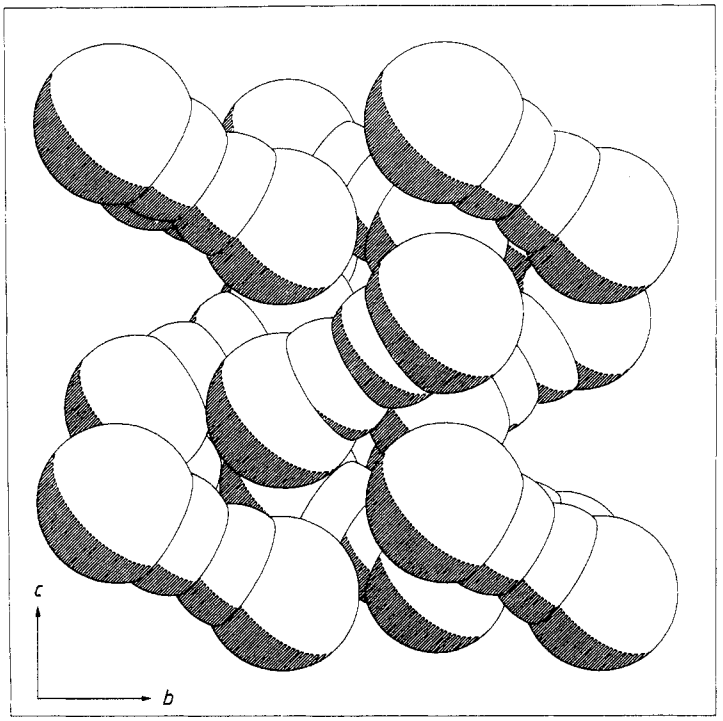

Figure 2. The structure of cyanogen at 15 K viewed down the *a* axis.

and the other two axes changed by less than −0.4%. Within the molecule, the bond lengths for C–C and C–N agree with the x-ray values within error limits and the molecule is linear within the same limits. In the earlier work on the lattice dynamics [2], parameters were adjusted to give equilibrium at 0 K and this gave a volume reduction of 5.2% and a *c*-axis reduction of 4% compared with the values at 178 K. It is now clear that these calculated reductions do not correspond to the true temperature dependence of the crystal structure.

5. Lattice dynamics

The lattice dynamics of cyanogen was recalculated using the new values of the lattice parameters, the atomic positions and the quadrupole moment. Standard potentials have been presented by Hirshfeld and Mirsky (HM) [3] and Williams and Cox (WC) [4] and, for reference purposes, we started with these potentials and calculated the equilibrium conditions, lattice energies and lattice frequencies. The van der Waals interactions were represented by

$$U(r) = A\,\mathrm{e}^{-\alpha r} - Br^{-6}$$

where A, B and α are adjustable parameters having distinct values for each of the three types of interaction, N–N, C–C and C–N. The computation included explicitly the interactions of a given molecule with its 18 nearest neighbours (an interaction range of 7.065 Å between molecular centres). The effects of more distant molecules were

Table 2. C_2N_2: a comparison of electrostatic energies (kJ mol^{-1} of dimer) for innermost shells.

Site	$U_{el}^{AM\,a}$	U_{el}^{b}	U_{el}^{c}
$\frac{1}{2}0\frac{1}{2}$	−2.982	−2.952	−3.034
$0\frac{1}{2}\frac{1}{2}$	−4.354	−4.210	−4.403
$\frac{1}{2}\frac{1}{2}0$	1.223	1.237	1.351
001	−1.402	−1.352	−1.448
100	0.308	0.326	0.383
010	−0.243	−0.240	−0.244
$\frac{1}{2}\frac{1}{2}1$	−0.126	−0.123	−0.145
$1\frac{1}{2}\frac{1}{2}$	−0.066	−0.066	−0.073
$\frac{1}{2}1\frac{1}{2}$	−0.258	−0.251	−0.267

[a] From [3]. The molecular charge density was decomposed into atomic fragments and each fragment was then represented by its calculated net charge, dipole and quadrupole moments localised at the atomic nuclei.

[b] The model described in the footnote a was simplified to include only dipoles. The magnitudes of the two independent dipoles were chosen to give the quadrupole and hexadecapole moments produced by the more complex model. The dipoles, one on each atom, are directed towards the centre of the molecule.

[c] These values were calculated using the same model as in footnote b but with the new structural parameters rather than the older x-ray results [1] used to calculate the results in the columns headed $U_{el}^{AM\,a}$ and U_{el}^{b}.

represented by a continuum approximation. This approximation was tested by including 48 neighbours in one calculation. The slight increase in accuracy did not warrant the increase in computation time.

The computer program, based on one originally developed by Pawley [10], was written to deal with dipole–dipole interactions so the electrostatic moments were represented by point dipoles oriented along the molecular axis, located on the four atoms and pointing towards the centre of the molecule. The magnitudes of the dipole moments were chosen to give the magnitudes of the quadrupole and hexadecapole moments calculated from HM's most detailed representation which included charges and dipole and quadrupole moments localised at the atomic nuclei. As a check on the adequacy of our model, the electrostatic interaction energies with various neighbours were calculated and compared with the values given by HM in their table 6 [3]. It can be seen from the results in table 2 that there is very little difference between the representations. Also listed in table 2 are the electrostatic interaction energies calculated with our new structural parameters.

The detailed changes in structure between the x-ray and neutron results are not nearly as important for the dynamics as are the changes in the quadrupole moment. This moment is measured to be $1.29e$ Å^2 ($6.2B$) compared with the $1.89e$ Å^2 ($9.1B$) used in the calculations described above. The electrostatic energy, which was comparable to the van der Waals energy in the earlier calculations, is reduced by about 50%. In table 3 are presented the results of the various calculations. Model A uses the HM potential parameters and the large dipole moments (to give $1.89e$ Å^2 for the quadrupole moment). Overall this model gives a fair match to the equilibrium conditions with the largest discrepancy being for the c direction. Lattice frequencies are calculated to be too low particularly at low frequencies. Model B is the same as model A except that the dipole moments have been scaled down to give a quadrupole moment of $1.29e$ Å^2. This scaling

Table 3. C_2N_2: calculated equilibrium conditions, observed and calculated lattice energies, lattice frequencies and quadrupole moments for various models. Model A: HM potential parameters and large dipoles; model B: HM potential parameters and small dipoles; model C: WC potential parameters and large dipoles; model D: WC potential parameters and small dipoles; model E: HM potential parameters, quadrupole as in A and hexadecapole set to zero; model F: HM potential parameters and dipoles varied to optimise the equilibrium conditions; model G: WC potential parameters and dipoles varied to optimise the equilibrium conditions; model H; potential parameters (9) and dipoles varied to optimise the fit to the listed experimental data.

Equilibrium conditions	Experiment	Model A	Model B	Model C	Model D	Model E	Model F	Model G	Model H
$(a/\Phi)\,\partial\Phi/\partial a = 0$		0.0014	−0.3219	−0.6423	−1.181	−2.329	0.059	−0.170	0.024
$(b/\Phi)\,\partial\Phi/\partial b = 0$		0.0813	−0.7220	−0.8340	−1.918	−1.604	−0.222	−0.397	−0.054
$(c/\Phi)\,\partial\Phi/\partial c = 0$		−0.2616	−0.6801	−0.9940	−1.655	−1.246	0.167	−0.361	0.020
$(1/\Phi)\,\partial\Phi/\partial\alpha = 0$		0.0840	0.0151	0.0597	−0.018	0.600	0.032	0.054	0.001
$(1/\Phi)\,\partial\Phi/\partial\beta = 0$		−0.0686	0.0581	0.0067	0.155	0.468	0.021	−0.054	0.004
$(1/\Phi)\,\partial\Phi/\partial\gamma = 0$		0.0136	−0.0402	0.0242	0.088	0.081	0.002	0.015	0.002
Crystal energy, Φ (kJ mol^{-1})	−40.4†	−29.4	−21.8	−30.6	−23.0	−27.2	−26.9	−37.4	−40.0
Lattice frequencies‡	44.5	26.5	2.3	20.9	16.5§	14.3	16.6	25.5	36.6
Librations (Raman) (cm^{-1})	58.5	39.1	32.0	43.9	36.1	40.8	37.4	48.5	50.0
	76	62.5	52.6	72.3	61.0	63.2	59.0	76.8	77.4
	79.5	64.9	58.2	77.2	69.0	82.8	68.3	84.4	81.4
	85	65.3	68.5	81.6	86.4	101.4	68.8	88.7	86.9
	109.5	90.0	87.0	109.0	107.1	117.5	92.6	118.3	113.1
	115	91.0	87.6	109.9	108.6	120.1	94.5	120.4	113.6
	115	93.6	89.5	112.7	109.8	130.2	95.9	122.0	117.4
Translations (infrared)	44	33.1	29.8	38.8	35.2	63.3	37.4	48.9	45.2
(cm^{-1})	72.5	63.3	61.4	76.9	75.3	68.7	61.4	76.1	67.6
	93.5	85.7	87.0	108.2	107.6	125.6	84.7	105.1	98.2
	108	95.2	88.1	113.1	109.2	131.4	90.8	115.0	100.0
	114.5	96.2	98.8	123.5	125.5	145.8	95.9	120.1	117.6
	114.5	105.2	111.0	135.7	140.3	155.5	108.0	133.2	120.6
Translations (inactive)	—	40.9	28.5	42.6	30.5	59.1	36.5	49.6	59.5
(cm^{-1})	—	60.9	56.3	72.4	68.7	90.6	58.8	74.4	65.3
	—	107.3	112.4	136.8	140.8	138.9	111.1	136.7	122.4
Quadrupole moment (e Å^2)	1.29	1.89	1.29	1.89	1.29	1.89	1.51	2.04	1.51
Hexadecapole moment (e Å^4)		9.98	6.82	9.98	6.82	0.0	5.01	6.45	8.12

† [11]. ‡ [12]. § Imaginary frequency.

process reduces the hexadecapole moment by the same percentage. Obviously the results obtained using model B are a much poorer match to the experimental results than those obtained with model A. Most of the equilibrium conditions are much more poorly satisfied. The crystal energy has dropped, so it is further from the experimental value, and the lattice frequencies, particularly the lowest one, are generally lower than with model A. Models C and D use the WC parameters with the large and small dipole moments, respectively. Neither of these models is as good as model A with the first three equilibrium conditions being particularly poorly satisfied. Lattice frequencies are too low at the low end and too high at the high end and for model D the lowest frequency is imaginary. Reducing the value of the dipole moment produces results that are generally further from the experimental ones.

An advantage of our simple dipole model is that it is easy to adjust the values of the quadrupole and hexadecapole moments separately. As a check on the importance of the hexadecapole moment, model A was modified to give model E in which the magnitude of the quadrupole moment is held fixed while the magnitude of the hexadecapole moment is set to zero. This has a very marked effect on the equilibrium conditions and also alters the frequencies by substantial amounts. Obviously a knowledge of the hexadecapole moment is important. There is no experimental value of this moment but the collision induced absorption measurements [13] limit its value to be less than 6 or 7e Å^4.

As a final test of the standard potentials, the magnitudes of the dipole moments were allowed to vary independently in order to minimise the deviations from the equilibrium conditions. The minimisation was done in a least-squares fashion using 500 iterations of a Simplex routine. The results are listed under models F and G of table 3 for the HM and WC potential parameters, respectively. These results show that variation of the dipole moments alone is not enough to produce a good fit to the experimental results. Finally, the nine potential parameters and the magnitudes of the two dipole moments were allowed to vary and the Simplex routine was used to give a least-squares fit to all of the experimental data listed in table 3. Lattice frequencies were fitted in ascending order for both librations and translations to avoid ambiguities in the assignments of the modes. The results are listed under model H of table 3. It is evident that this model gives the best overall agreement with the data.

The final potentials (from model H) are plotted in figure 3 along with the HM and WC potentials and the corresponding potential parameters are given in table 4. Our C–C potential is in reasonably good agreement with the earlier potentials but our N–N potential is quite different and our C–N potential is not related to our C–C and N–N potentials by the accepted combining rules.

6. Summary and conclusions

The new, low-temperature structural parameters presented in this paper and the recently measured quadrupole moment [5] have allowed a more stringent test of the models of the lattice dynamics to be made. Previous calculations have treated the lattice parameters as variables which is useful as a test for equilibrium but the deficiencies of the models are more obvious if the number of variables is kept to a minimum. The previously calculated variations of the lattice parameters are not consistent with the observed temperature dependence. The results given in table 2 show that a knowledge of both the quadrupole and hexadecapole moments is important, but that even allowing these moments to vary freely does not produce a good fit to the experimental results. A much

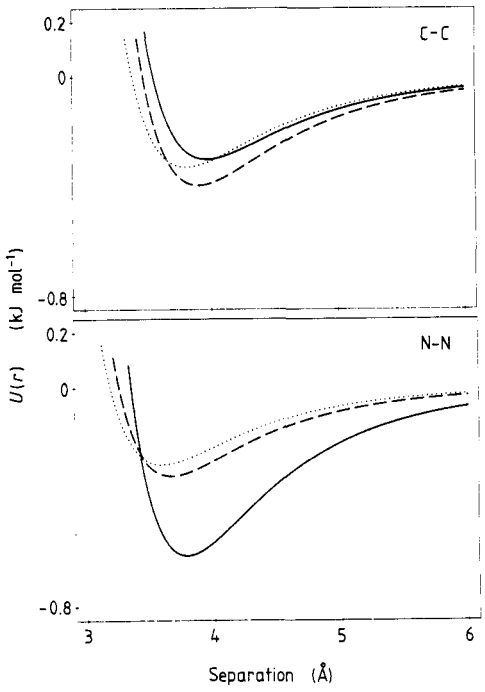

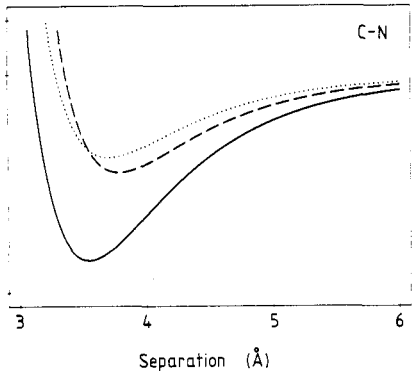

Figure 3. Our final potentials for cyanogen together with two standard potentials: ——, model H; · · · · ·, HM [3]; – – – –, WC [4].

Table 4. Potential parameters.

		A (kJ mol^{-1} Å^6)	B (10^5 kJ mol^{-1})	α (Å^{-1})
HM [3]	C–C	1761	3.00	3.68
	N–N	1084	1.76	3.78
	C–N	1382	2.30	3.73
WC [4]	C–C	2440	3.70	3.60
	N–N	1378	2.55	3.78
	C–N	1834	3.07	3.69
Model H	C–C	1967	6.57	3.78
	N–N	2733	0.93	3.33
	C–N	3232	3.45	3.56

improved fit is obtained if both potential parameters and the dipole moments are allowed to vary, but the final potentials thus obtained are quite different from the standard potentials available in the literature. One reason for the lack of transferability is the problem with electrostatic moments discussed above. For example, a reduction in the electrostatic energy produces a compensating increase in the potential well depths. A further reason is the fact that most of the crystal structures in the database used to derive the 'transferable' potentials have been determined at relatively high temperatures where anharmonic effects make a significant contribution. However, since the C–N potential is not close to being the geometric mean of the C–C and N–N potentials, the problems with the potentials are likely more fundamental.

The use of transferable potentials for the calculation of lattice dynamical vibrational frequencies has led to discrepancies with experimental data in other molecular solids. In d-benzene, Powell and co-workers [14] found that their inter-molecular mode frequencies could be equally well described by potential parameters very different from the 'accepted' transferable ones. The 'effective' parameters of Powell and co-workers [14] were viewed initially as 'physically unrealistic', but recent work [15] suggests that they are a better representation of d-benzene than those derived without the inclusion of the frequency data. A similar effect has recently been observed in sym-$C_6F_3Cl_3$, [16] where the inter-molecular-mode dispersion curves are described much better by a set of 'effective' potentials than by the accepted potentials derived using only electrostatic interactions and crystal structural data.

The present work adds to the increasing evidence that, even for molecules as simple as cyanogen, the concept of transferable, non-bonded potentials is not valid in its basic form. There are several possible developments that might restore the usefulness of the concept. A more elaborate description of the component terms of the total potential is perhaps required, lattice dynamical frequencies must be utilised as well as crystal structure data, and the latter must be measured at low temperatures to minimise possible anharmonic effects. All these effects will make it more difficult, both experimentally and theoretically, to derive potential parameters. Enough evidence of the failure of the concept in its simplest form has now been accumulated that all these developments should be included in the database if transferable, non-bonded potential parameters are possibly to remain a valid and useful concept.

Acknowledgments

Helpful discussions with Dr A Anderson are gratefully acknowledged. This research was supported in part by grants from the Natural Sciences and Engineering Research Council of Canada. The authors thank H F Nieman for expert preparation of the powder sample.

References

[1] Parkes A S and Hughes R E 1963 *Acta Crystallogr.* **16** 734–6
[2] Andrews B, McKenna J M, Anderson A and Leech J W 1984 *J. Phys. C: Solid State Phys.* **17** 3279–85
[3] Hirshfeld F L and Mirsky K 1979 *Acta Crystallogr.* A **35** 366–70
[4] Williams D E and Cox S R 1984 *Acta Crystallogr.* B **40** 404–17
[5] Dagg I R, Anderson A, Yan S, Smith W, Joslin C G and Read L A A 1986 *Can. J. Phys.* **64** 1475–81
[6] Nieman H F, Evans J C, Heal K M and Powell B M 1984 *J. Appl. Crystallogr.* **17** 372
[7] Pawley G S 1980 *J. Appl. Crystallogr.* **13** 630–3
[8] Rietveld H M 1969 *J. Appl. Crystallogr.* **2** 65–71
[9] Hewat A W 1979 *Acta Crystallogr.* A **35** 248
[10] Pawley G S 1972 *Phys. Status Solidi* b **49** 475–88
[11] Ruehrwein R A and Giauque W F 1939 *J. Am. Chem. Soc.* **61** 2940–4
[12] Andrews B, Anderson A and Torrie B H 1984 *J. Raman Spectrosc.* **15** 67–70
[13] Dagg I R 1988 private communication
[14] Powell B M, Dolling G and Bonadeo H 1978 *J. Chem. Phys.* **69** 2428–33
[15] Shi X and Bartell L S 1988 *J. Phys. Chem.* **92** 5667–73
[16] Dove M T, Powell B M and Pawley G S, Chaplot S L and Mierzejewski A 1989 *J. Phys. Chem.* **90** 1918–23